Green Chemistry

PAPER

View Article Online
View Journal | View Issue

Cite this: *Green Chem.*, 2019, **21**, 5586

Kinetics and mechanism for hydrothermal conversion of polyhydroxybutyrate (PHB) for wastewater valorization†

Yalin Li ‡[a,b] and Timothy J. Strathmann *[a,b,c]

Conventional wastewater treatment processes can be tailored to recover organic carbon from wastewater as intracellular polyhydroxybutyrate (PHB) polymer granules while simultaneously meeting effluent discharge standards. Traditional applications of PHB as a bioplastic are hampered by its suboptimal properties (*e.g.*, brittle), lack of efficient and sustainable approaches for recovering PHB from cells, and concerns about wastewater-derived impurities. In this study, we report on the conversion of PHB and its monomer acids – 3-hydroxybutyric acid (3HBA) and crotonic acid (CA) – under hydrothermal conditions (in condensed water at elevated temperature and pressure) to form propylene, a valuable chemical intermediate that self-separates from water. PHB depolymerization results in a mixture of 3HBA and CA, which can interconvert *via* (de)hydration reactions that vary with prevailing reaction conditions. Further hydrothermal conversion of the monomer acids yields propylene and CO_2. Conversion of 3HBA occurs at lower temperatures than CA, and a new concerted dehydration-decarboxylation pathway is proposed, which differs from the sequential dehydration (3HBA to CA) and decarboxylation (CA to propylene and CO_2) pathway reported for dry thermal conversion. A kinetics network model informed by experimental results reveals that CA conversion to propylene and CO_2 proceeds predominantly *via* hydration to 3HBA followed by the concerted dehydration-decarboxylation pathway rather than by direct decarboxylation of CA. Demonstrative experiments using PHB-containing methanotrophic biomass show results consistent with the model, producing propylene at near-theoretical yields at lower temperatures than reported previously.

Received 20th July 2019,
Accepted 19th September 2019

DOI: 10.1039/c9gc02507c

rsc.li/greenchem

1. Introduction

Sustainable management of wastewater represents a major challenge for public utilities, in part, due to inefficiencies of the existing infrastructure. Most notably, conventional wastewater treatment facilities employ a combination of energy- and chemical-consuming processes to remove organic matters and excess nutrients. For example, energy intensive aeration processes are used to oxidize organic carbon to CO_2.[1,2] To address these challenges and flip the energy balance of wastewater treatment operations, alternative processes that can treat wastewater while simultaneously recovering valuable resources from the waste stream (*e.g.*, fuels and other valuable chemicals) are attracting growing attention.[3–5] Recent reports demonstrate that organic carbon in wastewater can be recovered and valorized as intracellular polyhydroxyalkanoate (PHA) biopolymer granules,[6–8] in particular polyhydroxybutyrate (PHB, PHA with C_4 monomers, Fig. 1).[9–11] For example, waste organic matters can be converted to volatile fatty acids through acidogenic fermentation, which can then be used to select PHA/PHB-accumulating bacteria and enrich their PHA/PHB contents;[6,7,12,13] alternatively, biogas generated from anaerobic digestion can be leveraged for PHB production by methanotrophic bacteria.[14–16] Both of these approaches have been demonstrated at pilot scale,[6,7,16] and harvested biomass from these processes have been shown to accumulate up to 50–90% PHA/PHB content on cell dry weight basis.[8,17,18] To date, most of the efforts have been limited to utilizing PHB as a bio-derived and biodegradable alternative to petroleum-derived plastics,[19–21] which requires PHB to be separated from the biomass and purified to high grade. Separation of PHB often involves toxic halogenated solvents (*e.g.*, chloroform, dichloro-

[a]*Department of Civil and Environmental Engineering, Colorado School of Mines, Golden, Colorado 80401, USA. E-mail: strthmnn@mines.edu; Tel: +1 (303) 384-2226*
[b]*Engineering Research Center for Re-inventing the Nation's Urban Water Infrastructure (ReNUWIt), Colorado School of Mines, Golden, Colorado 80401, USA*
[c]*National Bioenergy Center, National Renewable Energy Laboratory, Golden, Colorado 80401, USA*

†Electronic supplementary information (ESI) available. See DOI: 10.1039/c9gc02507c

‡Present Address: Institute for Sustainability, Energy, and Environment, University of Illinois at Urbana-Champaign, Urbana, IL 61801, USA.

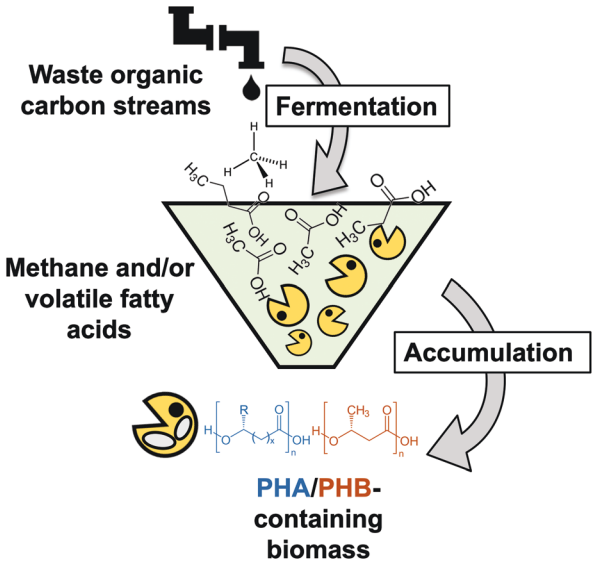

Fig. 1 Production of PHA (blue)/PHB (red) biopolymers from waste organic carbon streams.

methane) for high recovery and purity,[22] though use of green solvents (*e.g.*, methanol, propanol, acetic acid)[23] has been studied, their use at industrial scales can be very costly.[24] Other approaches including chemical/biological digestion, supercritical fluids extraction, and mechanical disruption have been explored, but these methods may lead to poor recovery or degradation of PHB, or they can be of high cost due to the multiple steps involved.[24] Further, the high cost of pure substrates (*e.g.*, glucose, glycerol)[25] for bio-synthesis of PHB diminishes the economic viability, and use of waste substrates is limited by concerns about carryover of impurities and toxic contaminants. Additionally, the brittle nature, low thermal stability, and weak durability of PHB also limit its practical use as a plastic substitute.[26,27]

Alternatively, recent efforts reveal that intracellular PHB granules can be converted to propylene – a valuable industrial chemical intermediate – when PHB-containing biomass is subjected to hydrothermal conditions (*i.e.*, in condensed water at elevated temperature and pressure).[28,29] Hydrothermal technologies are well-suited to process wet solids (80–90% moisture level) as they require much less energy for feedstock dewatering than complete drying needed by processes like pyrolysis. By leveraging the unique properties of water under hydrothermal conditions (*e.g.*, increased ion product promoting hydrolysis reactions, decreased dielectric constant leading to higher solubility of organic compounds[30,31]), PHB in the biomass can be converted to propylene that self-separates from the aqueous phase,[28,29] creating opportunities for efficient utilization of PHB and non-PHB cellular materials (NPCMs) that can be simultaneously converted to biocrudes and upgraded to hydrocarbon fuels.[32] Despite the relative high temperature and pressure (up to 350 °C and 30 MPa) involved in subcritical hydrothermal technologies,[31] existing studies on its application for algal biofuels indicate that the process can have overall beneficial impacts on the environment,[33,34] and the process can be economically competitive when low-cost waste-derived biomass feedstocks are used.[35,36] While previous studies observed propylene as a co-product of the biocrude oil formed during hydrothermal liquefaction (HTL) of PHB-containing biomass,[28,29] little is known about the controlling mechanism and process kinetics. Existing reports of PHB conversion have been limited mostly to pyrolysis (*i.e.*, pure PHB heated in absence of water or oxygen, also known as thermal decomposition),[37–40] and available reports[41] on PHB fate under hydrothermal conditions have focused on depolymerization reactions while further reactions of the resulting monomer acids – 3-hydroxybutyric acid (3HBA) and crotonic acid (CA) – have been largely ignored. The limited understanding of reaction kinetics and mechanism creates critical gaps in applying hydrothermal technologies for valorization of PHB-containing biomass, and should be addressed to evaluate the potential of such approaches for resource recovery from waste organic streams.

The objective of this work was to study the kinetics and mechanism of PHB conversion under hydrothermal conditions. Depolymerization of PHB and dehydration and decarboxylation of generated monomers 3HBA and CA were conducted at varying reaction temperatures (175–300 °C) with different initial reactant loadings (0.1–1 M) and amendments (acid, base, and salts of carboxylic acids). A new concerted dehydration-decarboxylation (DHYD-DCXY) mechanism was proposed for 3HBA and a reaction network was established with kinetics data used for deriving Arrhenius parameters for decomposition of 3HBA and CA. Conversion of PHB-containing biomass was demonstrated at milder conditions than previously reported and confirmed the identified mechanisms. Findings from this study provide important insights on hydrothermal conversion of biomass enriched in PHB and other polyhydroxyalkanoates (PHAs), thereby advancing a promising new strategy for enhanced valorization of organic components in wastewater.

2. Experimental

2.1. Depolymerization of model polyhydroxybutyrate (PHB)

Depolymerization of commercially sourced PHB (Sigma-Aldrich, natural origin in powder form) was conducted in stainless steel tube reactors (3/8″ outer diameter × 3″ length, 0.049″ wall thickness). Details on reactor construction are provided in the ESI, section S1, Fig. S1.† For each experiment, the desired mass (17.2–172.2 mg) of PHB was added to the reactor with 2 mL of aqueous solution (deionized water with or without amendments). The reactor was then sealed and immersed in a fluidized sand bath (Accurate Thermal Systems, FTBLL12) for desired reaction time, after which time the reactor was immersed in room-temperature water to rapidly terminate reactions. Autogenous pressure was maintained during the reaction (the maximum pressure was estimated to be around 2.3 MPa for 220 °C from saturated steam tables[42])

and was not expected to have major effects on the reaction.[43,44] Temperature-time profiles were measured with a thermocouple inserted inside a reactor containing 2 mL of water (Fig. S2† in the ESI). These measurements showed that <3 min was required to heat the reactor to the setpoint temperature or cool the reactor back to room temperature. After cooling, the reactor was opened and liquid contents were poured into a syringe attached with a 0.45 μm filter (cellulose acetate, Whatman®). The filtrate was then analyzed for monomer acids of PHB (3-hydroxybutyric acid, 3HBA and crotonic acid, CA). The reactor and syringe filter were dried at 65 °C before weighing, and the mass difference before and after reaction was used to estimate the quantity of residual PHB solids. A wide range of reaction conditions, including temperature (175, 200, 205, 210, 215, and 220 °C), initial PHB loading (0.1, 0.25, 0.5, 0.75, and 1 M as monomers), and various amendments (3HBA, CA, H_2SO_4, NaOH, and sodium salts of 3HBA, CA, butyric acid, and formic acid) were evaluated. All experiments were conducted at least in duplicate. Details on product analyses are provided in section S2 in the ESI.†

2.2. Conversion of PHB monomer acids to propylene

For experiments conducted using PHB monomer acids as starting materials, reactions were conducted in tube reactors sealed on one end with a bleed valve to enable gas sampling after quenching reactions (Fig. S1† in the ESI). For each experiment, 2 mL of aqueous solution prepared from the desired PHB-derived monomer acid was added to the reactor, which was then heated in the fluidized sand bath and quenched in the same manner described for depolymerization reactions. The maximum autogenous pressure was estimated to be around 8.6 MPa for 300 °C from saturated steam tables[42] and was not expected to have major effects on the reaction.[43,44] After cooling, the bleed valve was opened to collect headspace gas in a sampling bag (0.5 L ALTEF, Restek) for subsequent analysis. Gas product composition was analyzed for N_2, O_2, CO, CO_2, propylene and other volatile (C_1–C_6) hydrocarbons (analytical details provided in section S2 of the ESI†). Aqueous contents of the reactor were then collected and analyzed following the same procedures described for depolymerization reactions. Effects of temperature (200–275 °C for 3HBA and 225–300 °C for CA with 25 °C interval) and initial reactant loading (0.25, 0.5, and 0.75 M) were investigated. Kinetics data were typically collected at time 0.5, 1, 2, and 4 h, but sampling time for some reactions was adjusted to accommodate higher reaction rates.

2.3. Kinetics modeling

Reaction kinetics data collected from conversion of 3HBA and CA were modeled as a network of reactions following (pseudo-) first-order rate law, and a least-squares objective function (to minimize the sum of squared errors between experimental results and model predictions)[45] was used to calculate rate constants for individual reactions within the network model. Rate constants determined at varying temperatures were then used to estimate apparent activation energies (E_a, kJ mol^{-1}) and pre-exponential factors (A) according to the Arrhenius equation:

$$\ln k_{obs} = -\frac{E_a}{RT} + \ln A. \quad (1)$$

The Arrhenius parameters for each reaction in the network model were then applied to numerically calculate concentration timecourse profiles of each species to compare with experimental results for internal model validation.

2.4. Hydrothermal conversion of PHB-containing biomass

Demonstrative experiments were conducted using PHB-containing biomass relevant to wastewater treatment operations. The biomass was provided by Mango Materials (Albany, CA, USA) and was dried in an oven at 70 °C overnight and ground before analysis or use in experiments. PHB content of the biomass was measured by the supplier *via* acid methanolysis followed by gas chromatography analysis, C/H/N contents were measured by Huffman Hazen Laboratories (Golden, CO, USA), O content was estimated by difference (1-C%–H%–N%), and ash content was measured by calcination at 550 °C. Hydrothermal conversion of the biomass was conducted in the same reactors used for conversion of acid monomers. For each reaction, 86.1 mg of the biomass was mixed with 2 mL aqueous solution before sealing the reactor. The reactor was then heated to the designated temperature (250, 275, and 350 °C) and time (1–6 h depending on temperature) before quenching. Quantification and analyses of products followed the same protocols described above. Additional experiments were conducted at 250 °C for 4 h with H_2SO_4 as the amendment. A control experiment was conducted with PHB-containing biomass replaced by commercially sourced PHB to probe potential interactions between PHB and NPCMs in the biomass.

3. Results and discussion

3.1. Depolymerization of PHB

Hydrothermal reaction of PHB granules was first examined at mild conditions (175–220 °C) to provide insights into factors controlling depolymerization (Table 1). Minimal depolymerization was observed for reaction at 175 °C for 2 h, but a mixture of dissolved oligomers and monomers 3HBA and CA were observed when temperatures were increased to 200 °C. When temperature was further increased, more 3HBA and CA were generated with a concurrent reduction in residual PHB solid and oligomers, and almost no PHB remained after 2 h when temperature was ≥215 °C. Further, higher temperatures led to decreased carbon recovery (78.1 ± 1.1% at 220 °C *vs.* 91.9 ± 3.5% recovery for all reactions at 200 °C with varying PHB loading and amendments), which was expected to be a result of generated 3HBA and CA decomposing into gas products (discussed in section 3.2). The selectivity of monomer acids favored 3HBA at all temperatures ([3HBA]:[CA] around 2.1–3.1; Scheme 1). In addition, the initial PHB concentration (0.1–1 M) was found to have minimal effect on both the extent of depolymerization and selectivity of monomer products

Table 1 Hydrothermal depolymerization of PHB[a]

T (°C)	$[PHB]_0$ [b]	Aqueous solution	Yield[c] (C%) Residual PHB	Oligomers	3HBA	CA
Effect of Reaction Temperature						
175	0.5	DI water	98.6 ± 0.3%	0.7 ± 0.1%	0%	0%
200			55.3 ± 2.9%	23.3 ± 3.4%	10.5 ± 1.4%	3.5 ± 0.2%
205			42.6 ± 0.9%	28.4 ± 0.4%	15.8 ± 0.2%	5.2 ± 0.1%
210			23.4 ± 0.8%	26.9 ± 0.3%	27.4 ± 0.04%	9.2 ± 0.03%
215			0.9 ± 0.2%	24.2 ± 0.9%	38.0 ± 0.8%	18.2 ± 0.4%
220			1.4 ± 0.2%	16.5 ± 0.9%	41.1 ± 0.4%	19.2 ± 0.03%
Effect of Initial PHB Concentration						
200	0.1	DI water	52.9 ± 1.2%	24.0 ± 2.9%	9.4 ± 2.4%	2.7 ± 0.2%
	0.25		60.3 ± 6.9%	20.5 ± 4.9%	6.4 ± 1.8%	2.1 ± 0.4%
	0.5		55.3 ± 2.9%	23.3 ± 3.4%	10.5 ± 1.4%	3.5 ± 0.2%
	0.75		54.5 ± 2.5%	23.1 ± 3.9%	14.2 ± 1.5%	4.5 ± 0.4%
	1		54.4 ± 0.7%	20.6 ± 2.4%	11.2 ± 0.8%	3.6 ± 0.3%
Effect of Aqueous Medium						
200	0.5	DI water (pH_0[d] = 6.97)	55.3 ± 2.9%	23.3 ± 3.4%	10.5 ± 1.4%	3.5 ± 0.2%
		0.5 M 3HBA (pH_0 = 2.33)	34.5 ± 0.7%	0%	[e]	[e]
		0.5 M CA (pH_0 = 2.47)	12.8 ± 1.6%	0%	[e]	[e]
		0.005 M H_2SO_4 (pH_0 = 2.03)	47.8 ± 7.1%	19.9 ± 2.4%	17.2 ± 1.2%	1.7 ± 0.2%
		0.0005 M H_2SO_4 (pH_0 = 3.01)	73.3 ± 2.8%	15.5 ± 2.6%	4.6 ± 0.6%	1.0 ± 0.1%
		0.5 M Na_3HBA[f] (pH_0 = 7.00)	7.1 ± 1.3%	0%	[e]	[e]
		0.5 M NaCA[f] (pH_0 = 7.00)	10.6 ± 3.3%	0%	[e]	[e]
		0.5 M NaBA[f] (pH_0 = 7.02)	25.2 ± 7.3%	0%	22.0 ± 0.3%	56.9 ± 0.1%
		0.5 M NaFA[f] (pH_0 = 7.09)	0.6 ± 0.6%	0%	28.7 ± 0.7%	60.7 ± 2.6%
		0.5 M H_2SO_4 (pH_0 = 0)	0%	5.7 ± 4.7%	73.9 ± 2.4%	12.9 ± 0.3%
		1 M NaOH (pH_0 = 14)	1.4 ± 0.4%	9.2 ± 1.7%	53.9 ± 0.3%	33.3 ± 1.7%

[a] Reaction time was 2 h for all runs; all experiments were conducted in at least duplicate. [b] Initial PHB polymer loading as mol L^{-1} of monomers (solid/liquid). [c] Yields shown in carbon contents expressed as percentages of the initially loaded carbon. [d] pH of aqueous medium prior to reaction. [e] Concentration of 3HBA/CA species not shown due to their pre-existence in the initial aqueous reaction solution and difficulties in determining their origin (*i.e.*, from depolymerization of PHB or amendments). [f] Na3HBA, NaCA, NaBA, and NaFA refer to 3HBA, CA, butyric acid, and formic acid solutions neutralized with NaOH prior to reaction, respectively.

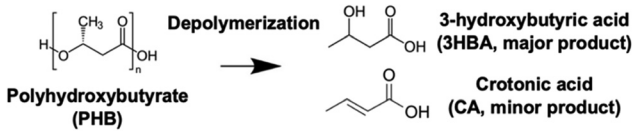

Scheme 1

(40–50% of PHB conversion after 2 h at 200 °C, 3HBA as the major product).

In contrast, changes in the aqueous medium composition did significantly influence both the rate of PHB depolymerization and the resulting selectivity of monomer acids. Amending the initial reaction solution with either monomer acid (3HBA or CA, 0.5 M) catalyzed PHB depolymerization, with the latter exerting a more pronounced effect (PHB depolymerization after 2 h increased from 44.7 ± 2.9% to 87.2 ± 1.6% when CA was added *vs.* 65.5 ± 0.7% when 3HBA was added). While addition of monomer acids lowered the initial pH of the solution (pH measurements were 2.33 and 2.47 for 0.5 M 3HBA and CA, respectively), acidification of the PHB mixture to the same pH range using H_2SO_4 had a much smaller effect on depolymerization, indicating that the monomer acids catalyzed PHB depolymerization *via* a mechanism other than increasing H^+ concentration. This conclusion was further supported by experiments showing near-complete depolymerization of PHB in solutions amended with 0.5 M 3HBA and CA that were neutralized to pH 7 before initiating the reaction. PHB depolymerization was also catalyzed in neutral-pH solutions amended with formate or butyrate salts (99.4 ± 0.6% and 74.8 ± 7.3% depolymerization after 2 h, respectively). Collectively, these findings indicate that the carboxyl group (–COOH/–COO^-) was instrumental in catalyzing PHB depolymerization, possibly *via* a mechanism similar to that proposed for pyrolysis reactions where cleavage of polyester bonds is initiated by attacking the α-hydrogen of the ester group (reaction (1)).[40] The higher reactivity of the deprotonated carboxylic acids was likely due to the greater bonding potential from absence of hydrogen.[38,40]

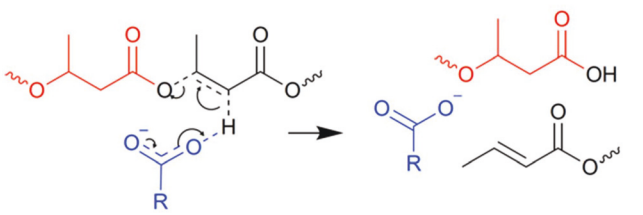

(1)

Although PHB depolymerization was observed under a variety of conditions, ratios of the resulting monomer acid

concentration – [3HBA] : [CA] – varied greatly. The observed ratios were relatively constant favoring 3HBA for reactions initiated in deionized water (3.0–3.5 for 0.1–1 M PHB reacted at 200 °C for 2 h). The ratio increased further to 4.7–10.3 when acidic solutions were introduced. In contrast, the ratio decreased to 1.6 for reaction in 1 N NaOH, and CA became the major product in reactions conducted in neutral-pH solutions amended with the sodium salts of formic or butyric acid (the ratio being 0.5 and 0.4, respectively). This was noteworthy as CA was reported to be the dominant monomer product observed for pyrolysis of PHB,[38,40] and selectivity of monomers has been largely overlooked in earlier reports of PHB depolymerization under hydrothermal conditions.

The variable monomer selectivity is consistent with multiple mechanisms controlling PHB depolymerization. Under acidic conditions, depolymerization may proceed predominantly *via* the reverse of Fischer esterification with 3HBA being the main product (reaction (2)):[46]

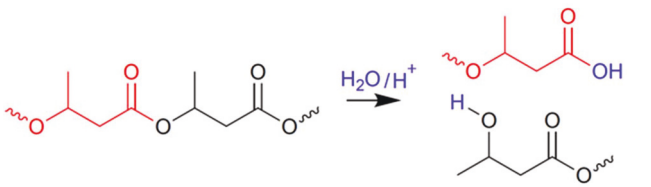

(2)

Under basic conditions, the reaction likely proceeds predominantly *via* the saponification pathway with salt of 3HBA being the main product (reaction (3)):[46,47]

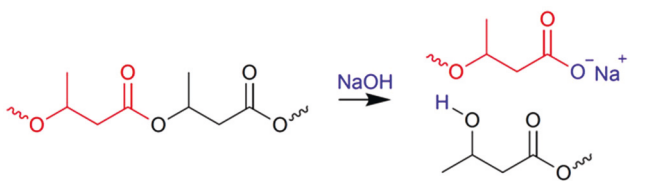

(3)

Meanwhile, under both acid and basic conditions, the generated carboxyl groups can further catalyze the depolymerization reaction *via* mechanism shown in reaction (1) (CA as the main product). As the deprotonated carboxyl terminal groups generated under basic conditions leads to faster reaction (1) than the protonated carboxyl terminal groups generated under acidic conditions (observed in earlier experiments), more CA (from reaction (1)) will be generated under basic conditions than under acid conditions, leading to a lower [3HBA] : [CA] ratio. It should be noted that under the investigated conditions, ion product of water could increase to 10^{-12}–10^{-11} $mol^2\ L^{-2}$ (2–3 orders of magnitude higher than at ambient condition),[30] which would significantly increase the concentrations of H^+ and OH^- and promote both acid- and base-catalyzed hydrolysis. However, the acid-catalyzed mechanism has been reported as the dominate one,[30] which may contribute to the higher selectivity toward 3HBA when water is used as the aqueous medium with no amendments. This link between amendments, controlling reaction mechanism, and [3HBA] : [CA] ratio is important as it allows for the selection of one monomer over the other, which can promote desired PHB-to-propylene conversion by selecting for the monomer acid that is more readily converted to propylene at lower reaction temperatures (section 3.2).

3.2. (De)hydration and decarboxylation of monomers

While 2 h reactions of PHB at temperatures ≤220 °C principally resulted in depolymerization to 3HBA and CA, reactions for longer times and/or higher temperatures led to further conversion of the monomer acids into propylene and CO_2. Thus, further experiments were then undertaken to specifically examine reactions of the two monomer acids that occurred under these conditions. In general, >90% of the initial carbon was recovered as 3HBA, CA, propylene, and CO_2, suggesting minimal side products and reactions.

3.2.1. Crotonic acid (CA). Preliminary experiments initiated with 0.5 M CA revealed no substantial production of propylene within 2 h at temperatures <250 °C, although around 10% of CA underwent hydration to 3HBA at the end of experiments, consistent with what was reported in literature (reaction (4)).[48]

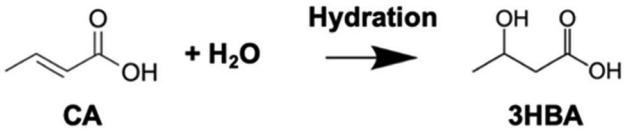

(4)

Increasing temperatures to ≥250 °C led to production of propylene and CO_2 at approximately theoretical ratios (1 : 1 on molar basis and 3 : 1 on carbon basis, Fig. 2), indicating onset of CA decarboxylation in addition to hydration (reaction (5)).

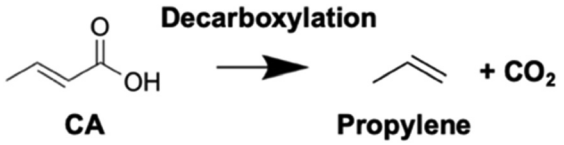

(5)

Reaction rates increased with temperature and near complete conversion of CA to propylene and CO_2 was observed within 4 h at 300 °C. 3HBA was observed as a transient intermediate (Fig. 2b) with peak concentrations occurring earlier and at lower maximum values with increasing temperature. This was expected to be the net result of CA hydration and subsequent 3HBA conversion (section 3.2.2). Separate experiments showed minimal influence of the initial CA concentration (0.25–0.75 M at 275 °C) on the apparent reaction kinetics and the resulting product selectivity, similar to PHB depolymerization.

3.2.2. 3-Hydroxybutyric acid (3HBA). Dehydration of 3HBA to CA was observed at temperatures ≥200 °C. The conversion of 3HBA to CA at low temperatures was expected as it had been reported as the initial step in 3HBA conversion during pyrol-

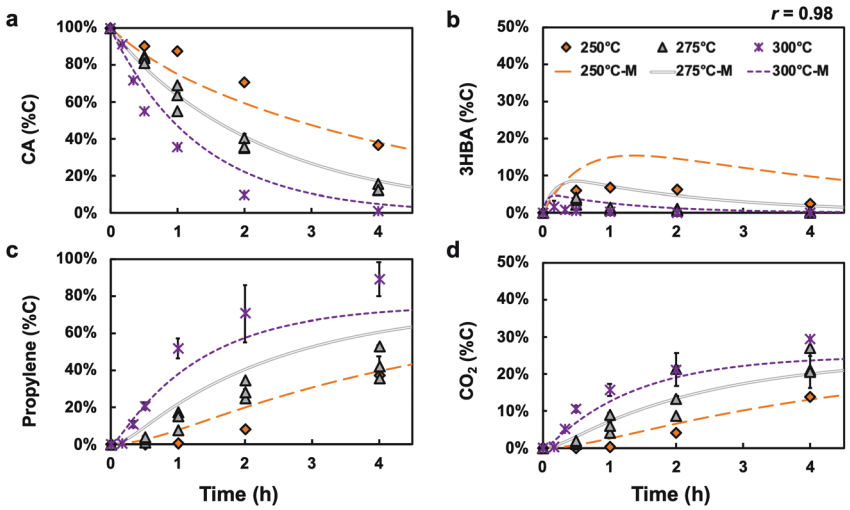

Fig. 2 Experimental measurements (discrete symbols) and model predictions (lines, eqn (2)–(5)) for conversion of 0.5 M CA at 250–300 °C. Yields are expressed as percentages of the initial loaded carbon. The Pearson correlation coefficient[49] *r* shown in the upper right evaluates the linear correlation between predicted values and experimental measurements for all points in a–d. Error bars for duplicate experiments represent min/max measured values and are smaller than symbols if not visible.

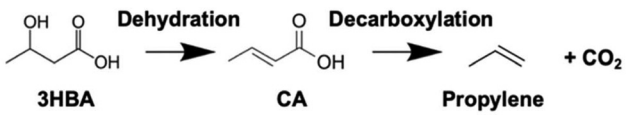

Scheme 2

ysis, which was proposed to be followed by decarboxylation of the generated CA to propylene and CO_2 (Scheme 2):[40]

Under hydrothermal conditions, 3HBA dehydration could follow the traditional E1 elimination mechanism with the *trans* isomer of CA being the dominant product (reaction (6)):

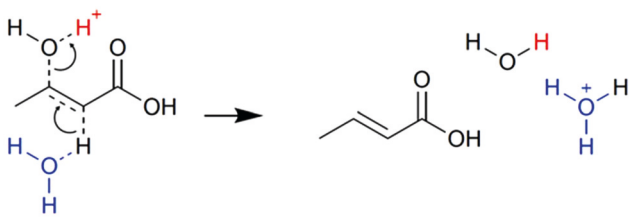

(6)

Based on the sequential reactions depicted in Scheme 2, gas production was not expected below 250 °C – the lowest temperature at which CA was observed to be converted into propylene and CO_2 as discussed in the previous section (Fig. 2c and d). It was thus not expected that >50% of 3HBA was converted to propylene and CO_2 (at the theoretical 1 : 1 molar ratio) when temperature was increased to 225 °C, with CA (from dehydration reaction) being a minor product. Therefore, decomposition of 3HBA to gas products occurred at lower temperatures and faster rates than CA (*i.e.*, rate of propylene and CO_2 formation from 3HBA at 225 °C > rate from CA at 250 °C). The inconsistency between this finding and the sequential dehydration and decarboxylation pathway (Scheme 2) suggests an alternative lower-temperature pathway for 3HBA conversion to propylene (section 3.3).

Experiments conducted at higher temperatures revealed a sharp increase in rates of 3HBA conversion. While only 20% of 3HBA was converted after 4 h of reaction at 200 °C, complete conversion was achieved within 0.5 h at 275 °C (Fig. 3a). Formation of the dehydration product CA also depended heavily on the temperature. For reactions at 200 and 225 °C, concentration of CA increased throughout the time studied; whereas for reactions conducted at 250 and 275 °C, CA concentration first increased to around 20% before decreasing (Fig. 3b). This can be explained by the net effects of CA formation by dehydration of 3HBA and decomposition of the generated CA to gas products. At 200 and 225 °C, 3HBA had not been fully converted within the time range monitored (4 h); but at 250 and 275 °C, all 3HBA had been converted within 1 h, and no additional CA was generated afterward. Meanwhile, further conversion of CA to propylene and CO_2 only became appreciable at ≥250 °C. In fact, concentration of CA started to decrease at 1 h for 250 °C and 0.5 h for 275 °C, corresponding with times at which 3HBA was nearly depleted. Likewise, rates of propylene and CO_2 production slowed after 3HBA was depleted, indicating that the faster 3HBA-to-gas pathway had ceased, but slower conversion of the residual CA continued (Fig. 3c and d). Finally, further tests showed that, like kinetics for PHB and CA conversion, the kinetics of 3HBA conversion were independent of its initial concentration (0.25–0.75 M at 225 °C).

3.3. Reaction mechanism

Synthesizing these observations together with the fact that no aqueous species other than 3HBA and CA were detected in sig-

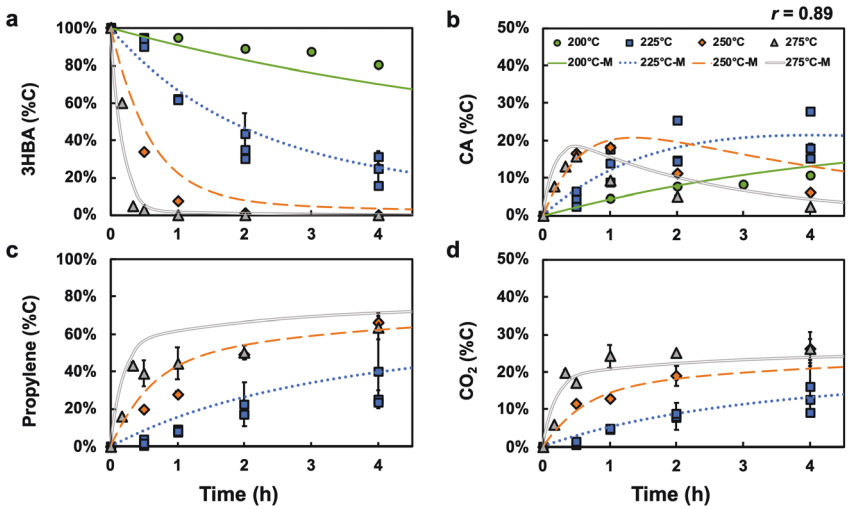

Fig. 3 Experimental measurements (discrete symbols) and model predictions (lines, eqn (2)–(5)) for conversion of 0.5 M 3HBA at 200–275 °C. Yields are expressed as percentages of the initial loaded carbon. The Pearson correlation coefficient[49] *r* shown in the upper right evaluates the linear correlation between predicted values and experimental measurements for all points in a–d. Error bars for duplicate experiments represent min/max measured values and are smaller than symbols if not visible.

nificant yields (>4%), a new mechanism was proposed for conversion of 3HBA to propylene and CO_2 (reaction (7)):

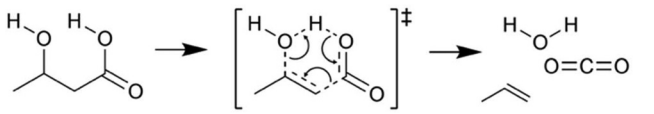

(7)

where dehydration and decarboxylation of 3HBA occurs in a concerted fashion (concerted DHYD-DCXY), thereby bypassing production of CA as an intermediate (Scheme 2, proposed mechanism for pyrolysis[40]). It is proposed that the reaction proceeds through an intramolecular 6-member ring transition state formed by hydrogen bonding between oxygen in the hydroxy group and hydrogen in the protonated carboxyl group. A similar mechanism has been proposed for decarboxylation of β-keto acids under hydrothermal conditions, where the cyclic transition state weakens the C–COOH bond (*e.g.*, decarboxylation of malonic acid shown in reaction (8)).[50–52]

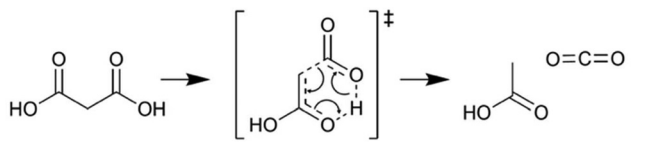

(8)

It should be noted that 3HBA must be protonated for the concerted reaction to proceed, which is supported by minimal (<2%) amounts of propylene and CO_2 formation when sodium salt of 3HBA was used as the initial reactant (225 and 275 °C, 0.5 M, 2 h).

As conversion of CA and generation of gas products followed (pseudo-) first-order rate law (Fig. 2), conversion of CA can either proceed through direct decarboxylation catalyzed by water (reaction (9)):

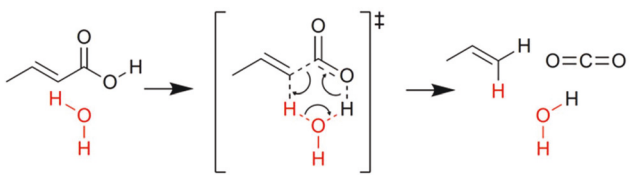

(9)

or through a two-step process where hydration to 3HBA is followed by concerted DHYD-DCXY of the generated 3HBA (Scheme 3):

For the direct decarboxylation route, hydrogen bonding with water forms a 6-member ring transition state that weakens the C–C bond between the carboxyl group and the α-carbon atom, leading to heterolytic cleavage and formation of the terminal alkene and CO_2. In fact, any molecules with a hydroxy group can catalyze the reaction *via* this proposed mechanism (*e.g.*, 3HBA from hydration of CA), but water is expected to be the main contributor due to its ubiquity at the studied conditions (molarity of water >100 times of CA for 0.5 M CA solution). Previous studies have reported the effects of water on decarboxylation reactions at similar conditions,[52–54] with computational studies suggesting water-involved cyclic transition state can lower the activation energy.[53,54] Similar to

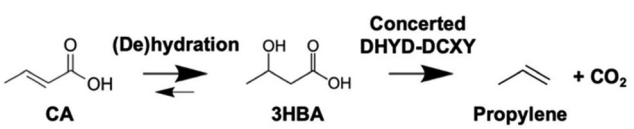

Scheme 3

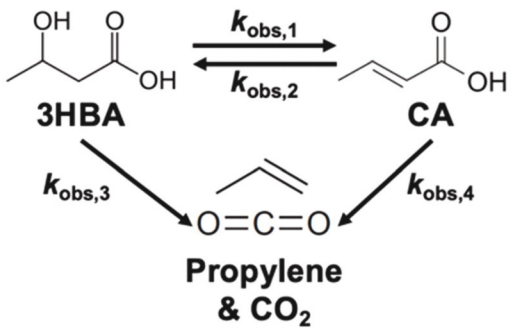

Scheme 4

the concerted DHYD-DCXY pathway of 3HBA, CA must be in its protonated form for the reaction to proceed *via* the proposed pathway in reaction (9), which is supported by the fact that <4% of propylene and CO_2 were observed during experiment initiated with the sodium salt of CA at 275 °C (0.5 M, 2 h). The relative importance of the two potential pathways for CA conversion to gas products was investigated with kinetics modeling (section 3.4).

To sum up, it is proposed that conversion of PHB monomers 3HBA and CA mainly proceed through four reactions: (1) dehydration of 3HBA to CA, (2) hydration of CA to 3HBA, (3) concerted DHYD-DCXY of 3HBA to propylene and CO_2, and (4) direct decarboxylation of CA to propylene and CO_2 (Scheme 4).

3.4. Kinetics model

A kinetics model was developed to provide quantitative support for the proposed reaction network depicted in Scheme 4. The kinetics of individual reactions were assumed to follow (pseudo-) first-order rate law, and concentration of each species (denoted as $[C_{Species}]$) expressed on carbon basis can be described as:

$$\frac{d[C_{3HBA}]}{dt} = -(k_{obs,1} + k_{obs,3})[C_{3HBA}] + k_{obs,2}[C_{CA}] \quad (2)$$

$$\frac{d[C_{CA}]}{dt} = -(k_{obs,2} + k_{obs,4})[C_{CA}] + k_{obs,1}[C_{3HBA}] \quad (3)$$

$$\frac{d[C_{Propylene}]}{dt} = \frac{3}{4}(k_{obs,3}[C_{3HBA}] + k_{obs,4}[C_{CA}]) \quad (4)$$

$$\frac{d[C_{CO_2}]}{dt} = \frac{1}{4}(k_{obs,3}[C_{3HBA}] + k_{obs,4}[C_{CA}]). \quad (5)$$

Next, least-squares objective function was used to fit the experimental data (concentration of 3HBA, CA, propylene, and CO_2 from conversion of 0.5 M 3HBA at 200–275 °C or 0.5 M CA at 250–300 °C) and determine values of the four apparent rate constants at each reaction temperature. The resulting "Fitted" rate constants are summarized in Table 2. Initially, all rate constants were freely adjusted during fits with the exception of $k_{obs,3}$ at 200 °C and $k_{obs,4}$ at 200 and 225 °C, which were fixed at 0 as minimal gas products were observed during experiments for 3HBA ($k_{obs,3}$) and CA ($k_{obs,4}$) reactions. However, the fit-derived values of $k_{obs,4}$ were found to negligible ($\leq$0.08 h^{-1}) compared to other rate constants, indicating that direct CA decarboxylation (reaction (9)) was not important and that the alternative pathway depicted in Scheme 3 (CA hydration to 3HBA followed by concerted DHYD-DCXY) predominated. As a result, model fitting was re-performed after excluding $k_{obs,4}$ for all reaction temperatures (*i.e.*, value fixed at 0). The resulting values of $k_{obs,1}$, $k_{obs,2}$, and $k_{obs,3}$ were similar to values determined when $k_{obs,4}$ was included during fitting (differences $\leq$0.11 h^{-1}), supporting elimination of the direct CA decarboxylation pathway from the reaction network.

Based on the results in Table 2, both dehydration and hydration reaction were slow at 200 °C, but the rate constant for CA hydration reaction ($k_{obs,2}$) was larger than that for 3HBA dehydration ($k_{obs,1}$), consistent with experimental results where more 3HBA was generated from CA (16.4 ± 0.6%) than CA from 3HBA (7.4 ± 0.3%). When temperature increased to 225 °C and above, however, the concerted DHYD-DCXY pathway predominated the consumption of 3HBA, with $k_{obs,3} \gg k_{obs,1}$ and $k_{obs,2}$. At 300 °C, reaction of 3HBA yielded negligible amounts of CA in comparison with propylene and CO_2, so $k_{obs,1}$ was excluded from the fit of data collected at this temperature.

The fitted (pseudo-) first-order rate constants for the 3HBA dehydration, CA hydration, and concerted DHYD-DCXY of

Table 2 Rate constants and fitted kinetics parameters[a]

k_{obs} [b] [h^{-1}]		T (°C)							
		200	225	250	275	300	E_a (kJ mol^{-1})	ln A	r^2
$k_{obs,1}$	Fitted	0.05 ± 0.01	0.14 ± 0.04	0.49 ± 0.05	1.16 ± 0.19	NA[c]	92.2 ± 3.4	20.4 ± 0.8	1.00
	Calculated	0.05	0.16	0.45	1.19	2.88			
$k_{obs,2}$	Fitted	0.12 ± 0.15	0.18 ± 0.17	0.26 ± 0.03	0.56 ± 0.01	1.03 ± 0.02	48.4 ± 5.5	10.0 ± 1.3	0.96
	Calculated	0.10	0.19	0.34	0.56	0.89			
$k_{obs,3}$	Fitted	NA[d]	0.25 ± 0.01	1.23 ± 0.03	3.18 ± 0.43	15.47 ± 0.81	126.8 ± 9.2	29.2 ± 2.1	0.99
	Calculated	0.05	0.25	1.08	4.07	13.69			

[a] Data for reactions of 0.5 M 3HBA or CA at different temperatures (Fig. 2 and 3) were fitted with eqn (2)–(5). [b] "Fitted" parameters were obtained by least-squares fitting with $k_{obs,3}$ at 200 °C and all $k_{obs,4}$ values fixed at 0 (negligible at the studied temperatures); "Calculated" parameters were calculated using Arrhenius parameters (eqn (1)), which were obtained by linear regression of the "Fitted" rate constant values (Fig. 4a). [c] Value fitted to be 0 by algorithm. [d] Value fixed at 0 during fitting because the reaction in question was not observed at this temperature.

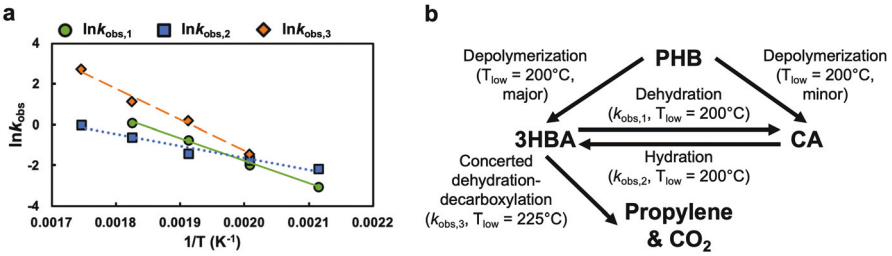

Fig. 4 (a) Fits of the Arrhenius equation (eqn (1)) for dehydration of 3HBA ($k_{obs,1}$), hydration of CA ($k_{obs,2}$), and concerted DHYD-DCXY of 3HBA ($k_{obs,3}$). The resulting activation parameters and fit qualities are provided in Table 2. (b) Proposed reaction network for PHB-to-propylene conversion. T_{low} indicates the lowest temperature at which each reaction was observed in this study.

3HBA reactions ($k_{obs,1}$ – $k_{obs,3}$) measured at 200–300 °C (Table 2, "Fitted" values) were used to derive apparent activation energies (E_a, kJ mol^{-1}) and pre-exponential factors (A) from least-squares fitting of the Arrhenius equation (eqn (1); Fig. 4a, Table 2). The Arrhenius parameters were then used to back-calculate rate constants at each temperature, including conditions where no rate constant could be directly observed (*e.g.*, $k_{obs,1}$ at 300 °C) (Table 2, "Calculated" values). The Arrhenius "Calculated" values generally agree closely with the "Fitted" values. Further validation of the kinetics network model and the Arrhenius activation parameters is provided by close agreement between measurements and predictions of the concentration profiles for CA, 3HBA, propylene and CO_2 measured at different temperatures (Pearson correlation coefficient[49] is 0.98 for CA and 0.89 for 3HBA, see model predictions in Fig. 2 and 3). For reactions initiated with 3HBA (Fig. 3), model predictions agree very closely with measurements for 3HBA at 225–275 °C, CA at 200 and 225 °C, propylene at 225 °C, and CO_2 at all temperatures were the most accurate with almost all points falling on or near the predicted lines. Some deviations were observed for 3HBA at 200 °C (underestimation), and CA (overestimation for >1 h) and propylene (overestimation 0.5–2 h) at 250–275 °C, but the deviations were not significant. Predictions for CA were even more robust with the only significant deviation being overprediction of 3HBA at 250 °C, which was probably due to the relative low concentrations of 3HBA forming at these conditions.

Fig. 4b summarizes the principal reaction pathways and lowest observed temperature (T_{low}) for each reaction. According to this reaction network, hydrothermal depolymerization of PHB occurs at temperatures ≥200 °C, with a predominance of 3HBA over CA (DI water as the aqueous medium without amendments). The monomer acids are interconvertible by (de) hydration reactions. At ≥225 °C, 3HBA is converted to propylene and CO_2 *via* the concerted DHYD-DCXY pathway, and experiments and modeling demonstrate that CA conversion to the same products occurs by sequential hydration to 3HBA followed by the concerted DHYD-DCXY pathway. These reactions occur at temperatures lower than those typically used for hydrothermal liquefaction of biomass for biocrude oil and co-products,[55] suggesting a strategy for selective production of propylene when hydrothermally processing PHB-containing biomass.

3.5. Conversion of PHB-containing biomass

As a demonstration and validation of the proposed reaction network, PHB-containing biomass was subjected to hydrothermal processing at conditions similar to those used for processing commercially sourced PHB and its monomer acids. The biomass was cultivated in a pilot-scale (500 L) reactor using natural gas as the methane source and was a mixed culture dominated by Type II methanotrophs. The biomass had a PHB content of 41.2 ± 0.7% with 51.9 ± 0.2% C, 7.2 ± 0.02% H, 5.0 ± 0.04% N, and 36.0 ± 0.2% O, and an ash content of 7.7 ± 0.2% (all on dry weight basis), which were comparable to those previously reported for methanotorphs.[10,56] Conversion was first conducted at 275 °C for 4 h since the kinetics model predicted that this condition would be sufficient for complete depolymerization of PHB and conversion of both 3HBA and CA to propylene and CO_2. As expected, all PHB in the biomass was converted to propylene and CO_2 at close-to-theoretical ratio (Table 3, Run 1). This was notable as previous reports of PHB-to-propylene were conducted at higher temperatures (300–375 °C for hydrothermal conversion,[28,29,57] 350–450 °C for pyrolysis[40,58]). Interestingly, when a higher reaction temperature was used, less propylene was observed despite complete conversion of PHB and its monomers (Table 3, Run 2), and the sum of 3HBA, CA, propylene, and CO_2 were only 74.3 ± 7.0% compared to 93.8 ± 7.5% at 275 °C. Since the yield of CO_2 remained unchanged, this was attributed to reactions between propylene and non-PHB cellular materials (NPCMs), or ketonization reactions between 3HBA/CA and NPCM derivatives that would generate CO_2 but not propylene.[32,59,60] Hydrothermal conversion of NPCMs may involve depolymerization of large biomacromolecules (*e.g.*, proteins to amino acids, triacylglycerides to fatty acids, carbohydrates to sugars), decomposition of the generated monomers (*e.g.*, decarboxylation, deamination, dehydration of amino acids), and further reactions between the monomers and derivative products (*e.g.*, amides from amino acids and fatty acid esters, melanoidins from Maillard reactions of amino acids and sugars).[59] Reactions between acids and alkenes (highly reactive due to the presence of carboxylic group and/or double bond) produced from hydrothermal conversion of medium chain-length PHA and NPCMs have

Table 3 Hydrothermal conversion of PHB-containing biomass[a]

Run #	T (°C)	t (h)	Aqueous medium	Yield[b] (C%)			
				3HBA	CA	Propylene	CO_2
1	275	4	DI water	0%	0%	69.5 ± 4.2%	24.3 ± 6.2%
2	350	1	DI water	0%	0%	53.5 ± 6.2%	20.8 ± 3.3%
3	250	2	DI water	5.0 ± 0.3%	36.6 ± 2.0%	38.2 ± 2.6%	13.2 ± 0.1%
4	250	4	DI water	2.7 ± 0.4%	20.1 ± 1.4%	54.0 ± 2.2%	19.4 ± 2.2%
5	250	6	DI water	2.5 ± 0.2%	14.3 ± 1.6%	61.4 ± 4.9%	23.6 ± 1.2%
6	250	4	0.005 M H_2SO_4	2.6 ± 0.1%	20.3 ± 0.8%	42.5 ± 12.8%	15.5 ± 3.8%
7	250	4	0.05 M H_2SO_4	3.5 ± 0.1%	30.5 ± 0.4%	37.8 ± 2.2%	13.3 ± 1.5%
8	250	4	DI water	2.4 ± 0.2%	28.9 ± 0.3%	35.6 ± 3.3%	10.1 ± 1.1%

[a] All experiments were started with 86.1 mg of solids and 2 mL of aqueous solution, which was an equivalent of 0.5 M (as PHB monomers) assuming the solid was 100% PHB; PHB-containing biomass was used for Runs 1–7 and commercially sourced PHB was used for Run 8. All experiments were performed in duplicate. [b] Yields shown in carbon contents expressed as percentages of initially loaded PHB.

been observed, but mechanisms of these reactions have not been examined.[32] It follows that lower reaction temperatures not only reduce heating energy requirements, but also maximize propylene yields by reducing losses to biocrude/aqueous products due to reactions with NPCM derivatives.

Experiments were then conducted at 250 °C to gauge the potential for further lowering reaction temperatures. Within 2 h, half of the intracellular PHB had decomposed to propylene and CO_2 with near-complete conversion of 3HBA, but around 40% of CA remained (Table 3, Run 3). When the reaction was extended to 4 and 6 h, the CA gradually decomposed and around 80% of the initial PHB was converted to propylene and CO_2 (Table 3, Runs 4 and 5). To further accelerate the conversion *via* the faster concerted DHYD-DCXY of 3HBA, additional experiments were also performed with acid solution as the aqueous medium instead of water, as earlier data revealed higher selectivity to 3HBA during depolymerization of PHB under acidic conditions. However, use of acid solutions decreased rates of PHB conversion and yields of propylene and CO_2 (Table 3, Runs 6 and 7), and the sum of 3HBA, CA, propylene, and CO_2 decreased to 80–85%, indicating potential loss to interactions with NPCM derivatives that can be catalyzed by the added acids.[61] Interestingly, experiments also showed that intracellular PHB was depolymerized more rapidly than commercially sourced PHB granules subjected to the same hydrothermal conditions (Table 3, Runs 4 and 8), and the sum of 3HBA, CA, propylene, and CO_2 for pure PHB was only 77.0 ± 3.5%, suggesting incomplete conversion of oligomers and slower kinetics. The faster conversion of intracellular PHB might be a result of its amorphous elastomeric state,[62] which can be lost upon extraction from the cells;[63] or due to the interactions between the intracellular PHB, its monomers, and NPCMs that either favors production of 3HBA (from depolymerization of PHB or hydration of CA) or inhibits the dehydration of 3HBA to CA. These results highlight the needs to examine the role of NPCMs and their derivatives in hydrothermal conversion of PHB at varying conditions and corresponding mechanisms, which should be addressed in future research. Still, findings from this work demonstrate effective conversion of intracellular PHB to near-theoretical yields of propylene at temperatures significantly lower than past reports. This provides a promising pathway forward for enhanced valorization of wastewater organic carbon sources.

3.6. Broader impacts

With waste valorization through biorefineries attracting increased attention,[64–66] there is growing interest in identifying promising strategies for resource recovery from waste organic streams.[2,3,67] Herein, hydrothermal conversion of wastewater-derived PHB is proposed for generation of propylene, which in turn can be used for production of liquid fuels (*e.g.*, C_6–C_{12} hydrocarbons *via* oligomerization[68]) or other higher-value chemicals (*e.g.*, cumene,[69] propanediol[70]). As the market for propylene is projected to grow in the future and North America is predicted to be one of the largest markets,[71] wastewater is an appealing source to meet these demands in a more sustainable and cost-effective manner. With developments in biocatalysts, polyhydroxyalkanoates (PHAs) with higher molecular weight monomers (*e.g.*, polyhydroxyvalerate[72]) can also be synthesized. Under hydrothermal conditions, these PHAs are expected to go through similar reactions: the depolymerization and (de)hydration pathways are viable for all PHAs and their monomers, and the concerted DHYD-DCXY pathway is viable for any PHA monomers containing a β-hydroxy group, which are commonly produced by microorganisms.[73] Therefore, longer renewable alkenes with broader applications could be produced in a similar manner.[32] In addition, the concerted DHYD-DCXY pathway is particularly interesting as it provides the possibility to bypass direct decarboxylation of unsaturated carboxylic acids, which proceeds at much lower rates compared to saturated fatty acids.[65,74] Moreover, mechanistic insights concluded in this study can be applied to determine optimal reaction conditions for converting PHB-containing biomass. The lower reaction temperatures are not only beneficial in reducing capital and operating costs, but also result in higher propylene yields by avoiding the incorporation of propylene into biocrudes or aqueous products generated from hydrothermal liquefaction of NPCMs.

4. Conclusions

In this work, hydrothermal conversion of PHB and its monomers 3HBA and CA were studied for production of propylene from wastewater-derived biomass. It was concluded that under hydrothermal conditions, PHB would first depolymerize into a mixture of 3HBA and CA, which would dehydrate and decarboxylate into propylene and CO_2. Selectivity of PHB depolymerization was found to be greatly affected by aqueous media: while 3HBA was the major product in water without amendments or with addition of mineral acids, addition of mineral base decreased the selectivity to 3HBA, and CA would become the major product with carboxyl amendments. This variation in product selectivity was attributed to the dominate depolymerization mechanism that varied with aqueous amendments but not with initial PHB loading nor reaction temperature. Further investigation of 3HBA and CA decomposition revealed that 3HBA could be converted to propylene at lower temperatures and faster rates than CA, and a new concerted DHYD-DCXY pathway was proposed for 3HBA. A kinetics network model was developed for conversion of PHB and Arrhenius kinetics parameters were derived for decomposition of 3HBA and CA, which revealed that conversion of CA to propylene proceeded mainly through hydration to 3HBA followed by the concerted DHYD-DCXY pathway. Conversion of PHB-containing biomass was demonstrated at conditions that were milder than previously reported, and near-theoretical production of propylene was observed, validating conclusions from the kinetics study and the developed network model.

Conflicts of interest

There are no conflicts to declare.

Acknowledgements

Financial support for work carried out at CSM was provided by National Science Foundation (NSF) through the NSF Engineering Research Center for Reinventing the Nation's Urban Water Infrastructure (ReNUWIt; EEC-1028968) and NSF award CBET-1804513. Derek Vardon (National Renewable Energy Laboratory) is acknowledged for valuable discussions. Allison Pieja and Yu Kuwabara at Mango Materials are acknowledged for providing PHB-containing biomass.

References

1 U.S. EPA, *Energy Efficiency in Water and Wastewater Facilities*, 2013.
2 W.-W. Li, H.-Q. Yu and B. E. Rittmann, *Nat. News*, 2015, **528**, 29.
3 M. T. Agler, B. A. Wrenn, S. H. Zinder and L. T. Angenent, *Trends Biotechnol.*, 2011, **29**, 70–78.
4 R. Kleerebezem, B. Joosse, R. Rozendal and M. C. M. van Loosdrecht, *Rev. Environ. Sci. Biotechnol.*, 2015, **14**, 787–801.
5 K. Solon, E. I. P. Volcke, M. Spérandio and M. C. M. van Loosdrecht, *Environ. Sci.: Water Res. Technol.*, 2019, **5**, 631–642.
6 S. Bengtsson, A. Karlsson, T. Alexandersson, L. Quadri, M. Hjort, P. Johansson, F. Morgan-Sagastume, S. Anterrieu, M. Arcos-Hernandez, L. Karabegovic, P. Magnusson and A. Werker, *New Biotechnol.*, 2017, **35**, 42–53.
7 F. Morgan-Sagastume, M. Hjort, D. Cirne, F. Gérardin, S. Lacroix, G. Gaval, L. Karabegovic, T. Alexandersson, P. Johansson, A. Karlsson, S. Bengtsson, M. V. Arcos-Hernández, P. Magnusson and A. Werker, *Bioresour. Technol.*, 2015, **181**, 78–89.
8 E. Korkakaki, M. Mulders, A. Veeken, R. Rozendal, M. C. M. van Loosdrecht and R. Kleerebezem, *Water Res.*, 2016, **96**, 74–83.
9 H. Salehizadeh and M. C. M. van Loosdrecht, *Biotechnol. Adv.*, 2004, **22**, 261–279.
10 A. J. Pieja, E. R. Sundstrom and C. S. Criddle, *Appl. Environ. Microbiol.*, 2011, **77**, 6012–6019.
11 K. Khosravi-Darani, Z.-B. Mokhtari, T. Amai and K. Tanaka, *Appl. Microbiol. Biotechnol.*, 2013, **97**, 1407–1424.
12 N. Basset, E. Katsou, N. Frison, S. Malamis, J. Dosta and F. Fatone, *Bioresour. Technol.*, 2016, **200**, 820–829.
13 N. Frison, E. Katsou, S. Malamis, A. Oehmen and F. Fatone, *Environ. Sci. Technol.*, 2015, **49**, 10877–10885.
14 P. J. Strong, S. Xie and W. P. Clarke, *Environ. Sci. Technol.*, 2015, **49**, 4001–4018.
15 P. J. Strong, M. Kalyuzhnaya, J. Silverman and W. P. Clarke, *Bioresour. Technol.*, 2016, **215**, 314–323.
16 A. J. Pieja, M. C. Morse and A. J. Cal, *Curr. Opin. Chem. Biol.*, 2017, **41**, 123–131.
17 S. Bengtsson, A. Werker, M. Christensson and T. Welander, *Bioresour. Technol.*, 2008, **99**, 509–516.
18 J. Tamis, K. Lužkov, Y. Jiang, M. C. M. van Loosdrecht and R. Kleerebezem, *J. Biotechnol.*, 2014, **192**(Part A), 161–169.
19 E. Akaraonye, T. Keshavarz and I. Roy, *J. Chem. Technol. Biotechnol.*, 2010, **85**, 732–743.
20 S. Chanprateep, *J. Biosci. Bioeng.*, 2010, **110**, 621–632.
21 K. Dietrich, M.-J. Dumont, L. F. Del Rio and V. Orsat, *Sustain. Prod. Consumption*, 2017, **9**, 58–70.
22 N. Jacquel, C.-W. Lo, Y.-H. Wei, H.-S. Wu and S. S. Wang, *Biochem. Eng. J.*, 2008, **39**, 15–27.
23 A. Aramvash, F. M. Zavareh and N. G. Banadkuki, *Eng. Life Sci.*, 2018, **18**, 20–28.
24 C. Pérez-Rivero, J. P. López-Gómez and I. Roy, *Biochem. Eng. J.*, 2019, **150**, 107283.
25 J. Możejko-Ciesielska and R. Kiewisz, *Microbiol. Res.*, 2016, **192**, 271–282.
26 J. Yu and L. X. L. Chen, *Biotechnol. Prog.*, 2006, **22**, 547–553.
27 P. J. Strong, B. Laycock, S. N. S. Mahamud, P. D. Jensen, P. A. Lant, G. Tyson and S. Pratt, *Microorganisms*, 2016, **4**, 11.

28 J. Wagner, R. Bransgrove, T. A. Beacham, M. J. Allen, K. Meixner, B. Drosg, V. P. Ting and C. J. Chuck, *Bioresour. Technol.*, 2016, **207**, 166–174.
29 C. Torri, T. D. O. Weme, C. Samorì, A. Kiwan and D. W. F. Brilman, *Environ. Sci. Technol.*, 2017, **51**, 12683–12691.
30 N. Akiya and P. E. Savage, *Chem. Rev.*, 2002, **102**, 2725–2750.
31 P. E. Savage, *J. Supercrit. Fluids*, 2009, **47**, 407–414.
32 T. Dong, W. Xiong, J. Yu and P. T. Pienkos, *RSC Adv.*, 2018, **8**, 34380–34387.
33 C. M. Beal, L. N. Gerber, D. L. Sills, M. E. Huntley, S. C. Machesky, M. J. Walsh, J. W. Tester, I. Archibald, J. Granados and C. H. Greene, *Algal Res.*, 2015, **10**, 266–279.
34 L. N. Gerber, J. W. Tester, C. M. Beal, M. E. Huntley and D. L. Sills, *Environ. Sci. Technol.*, 2016, **50**, 3333–3341.
35 S. Leow, B. D. Shoener, Y. Li, J. L. DeBellis, J. Markham, R. Davis, L. M. L. Laurens, P. T. Pienkos, S. M. Cook, T. J. Strathmann and J. S. Guest, *Environ. Sci. Technol.*, 2018, **52**, 13591–13599.
36 Y. Li, W. A. Tarpeh, K. L. Nelson and T. J. Strathmann, *Environ. Sci. Technol.*, 2018, **52**, 12717–12727.
37 S. Nguyen, G. Yu and R. H. Marchessault, *Biomacromolecules*, 2002, **3**, 219–224.
38 H. Ariffin, H. Nishida, Y. Shirai and M. A. Hassan, *Polym. Degrad. Stab.*, 2008, **93**, 1433–1439.
39 H. Nishida, H. Ariffin, Y. Shirai and M. Hassan, in *Biopolymers*, ed. M. Elnashar, Sciyo, 2010, ch. 19, pp. 369–386.
40 J. M. Clark, H. M. Pilath, A. Mittal, W. E. Michener, D. J. Robichaud and D. K. Johnson, *J. Phys. Chem. A*, 2016, **120**, 332–345.
41 T. Saeki, T. Tsukegi, H. Tsuji, H. Daimon and K. Fujie, *Polymer*, 2005, **46**, 2157–2162.
42 W. M. Haynes, *CRC Handbook of Chemistry and Physics*, CRC Press, 97th edn, 2016.
43 A. G. Carr, R. Mammucari and N. R. Foster, *Chem. Eng. J.*, 2011, **172**, 1–17.
44 J. L. Faeth, P. J. Valdez and P. E. Savage, *Energy Fuels*, 2013, **27**, 1391–1398.
45 D. C. Harris, *J. Chem. Educ.*, 1998, **75**, 119.
46 J. Yu, D. Plackett and L. X. L. Chen, *Polym. Degrad. Stab.*, 2005, **89**, 289–299.
47 N. F. S. M. Farid, H. Ariffin, M. R. Z. Mamat, M. A. K. M. Zahari and M. A. Hassan, *RSC Adv.*, 2015, **5**, 33546–33553.
48 D. Pressman and H. J. Lucas, *J. Am. Chem. Soc.*, 1939, **61**, 2271–2277.
49 J. Benesty, J. Chen, Y. Huang and I. Cohen, in *Noise reduction in speech processing*, Springer, 2009, pp. 1–4.
50 G. A. Hall, *J. Am. Chem. Soc.*, 1949, **71**, 2691–2693.
51 P. G. Maiella and T. B. Brill, *J. Phys. Chem.*, 1996, **100**, 14352–14355.
52 A. J. Belsky, P. G. Maiella and T. B. Brill, *J. Phys. Chem. A*, 1999, **103**, 4253–4260.
53 I. Lee, J. K. Cho and B.-S. Lee, *J. Chem. Soc., Perkin Trans. 2*, 1988, 1319–1323.
54 J. M. Clark, M. R. Nimlos and D. J. Robichaud, *J. Phys. Chem. A*, 2015, **119**, 501–516.
55 D. C. Elliott, B. Patrick, A. B. Ross, A. J. Schmidt and S. B. Jones, *Bioresour. Technol.*, 2015, **178**, 147–156.
56 K.-D. Wendlandt, M. Jechorek, J. Helm and U. Stottmeister, *J. Biotechnol.*, 2001, **86**, 127–133.
57 C. R. Fischer, A. A. Peterson and J. W. Tester, *Ind. Eng. Chem. Res.*, 2011, **50**, 4420–4424.
58 H. Pilath, A. Mittal, L. Moens, T. B. Vinzant, W. Wang and D. K. Johnson, in *Direct Microbial Conversion of Biomass to Advanced Biofuels*, ed. M. E. Himmel, Elsevier, Amsterdam, 2015, pp. 383–394.
59 S. M. Changi, J. L. Faeth, N. Mo and P. E. Savage, *Ind. Eng. Chem. Res.*, 2015, **54**, 11733–11758.
60 S. Kang and J. Yu, *RSC Adv.*, 2015, **5**, 30005–30013.
61 A. B. Ross, P. Biller, M. L. Kubacki, H. Li, A. Lea-Langton and J. M. Jones, *Fuel*, 2010, **89**, 2234–2243.
62 L. Martino, M. V. Cruz, A. Scoma, F. Freitas, L. Bertin, M. Scandola and M. A. M. Reis, *Int. J. Biol. Macromol.*, 2014, **71**, 117–123.
63 G. N. Barnard and J. K. Sanders, *J. Biol. Chem.*, 1989, **264**, 3286–3291.
64 J. G. Linger, D. R. Vardon, M. T. Guarnieri, E. M. Karp, G. B. Hunsinger, M. A. Franden, C. W. Johnson, G. Chupka, T. J. Strathmann, P. T. Pienkos and G. T. Beckham, *Proc. Natl. Acad. Sci. U. S. A.*, 2014, **111**, 12013–12018.
65 D. R. Vardon, B. K. Sharma, H. Jaramillo, D. Kim, J. K. Choe, P. N. Ciesielski and T. J. Strathmann, *Green Chem.*, 2014, **16**, 1507–1520.
66 D. Kim, D. R. Vardon, D. Murali, B. K. Sharma and T. J. Strathmann, *ACS Sustainable Chem. Eng.*, 2016, **4**, 1775–1784.
67 G. W. Roberts, M.-O. P. Fortier, B. S. M. Sturm and S. M. Stagg-Williams, *Energy Fuels*, 2013, **27**, 857–867.
68 J. Q. Bond, D. M. Alonso, D. Wang, R. M. West and J. A. Dumesic, *Science*, 2010, **327**, 1110–1114.
69 T. F. Degnan, C. M. Smith and C. R. Venkat, *Appl. Catal., A*, 2001, **221**, 283–294.
70 J. O. Metzger, *Eur. J. Lipid Sci. Technol.*, 2009, **111**, 865–876.
71 IHS Markit, Chemical Economics Handbook (CEH) – Propylene, https://ihsmarkit.com/products/propylene-chemical-economics-handbook.html, (accessed December 6, 2018).
72 C. T. Nomura and S. Taguchi, *Appl. Microbiol. Biotechnol.*, 2007, **73**, 969–979.
73 Z. A. Raza, S. Abid and I. M. Banat, *Int. Biodeterior. Biodegrad.*, 2018, **126**, 45–56.
74 J. Fu, X. Lu and P. E. Savage, *ChemSusChem*, 2011, **4**, 481–486.